J Mater Sci (2009) 44:3077–3081
DOI 10.1007/s10853-009-3409-8

Mechanical response of the TiAl/steel brazed joint under impact load

Yulong Li · Jicai Feng · He Peng · Zhang Hua

Received: 8 November 2008 / Accepted: 16 March 2009 / Published online: 7 April 2009

Abstract Mesnager impact tests of TiAl base metal and TiAl/steel brazed joints were conducted at room temperature (293 K) and elevated temperature (623 K). Impact strength, impact energy, fracture path, and the behavior of the reaction phases were studied. For the room temperature test, average impact energy and strength of the joint are 71.9% and 84.2% of the TiAl base metal, respectively; which are 62.5% and 75.3% of TiAl base metal, respectively, at 623 K. Fracture path and crack propagation process analysis show, when subjected to the impact load, cracks germinate at the interface of Ag-based solid solution/$AlCu_2Ti$ particles, grow up and propagate into the Al–Cu–Ti brittle reaction layers, then propagate into the TiAl base metal, and result in failure.

Y. Li (✉) · Z. Hua
Key Lab for Robot & Welding Automation of Jiangxi Province, Nanchang University, Nanchang 330031, People's Republic of China
e-mail: liyulong1112ster@gmail.com

Z. Hua
e-mail: zhanghua_dr@163.com

Y. Li · J. Feng · H. Peng
State Key Laboratory of Advanced Welding Production Technology, Harbin Institute of Technology, Harbin 150001, People's Republic of China

J. Feng
e-mail: fengjc@hope.hit.edu.cn

H. Peng
e-mail: hepeng@hope.hit.edu.cn

Introduction

TiAl-based alloy is regarded as one of the candidates for high temperature usage especially in advanced automobile and aircraft engine components because of its low density, high melting temperature, and high temperature strength [1–4]. In the recent years, the investigations about the commercial application of TiAl-based alloy involved many aspects [5–8], in which a technology of joining TiAl with other structural materials became popular. Particularly, the technology of joining TiAl and structural steels with excellent toughness is required for engine turbo components [9–11]. Utilizing a TiAl turbine/steel shaft structure as the turbine rotor, during service the joint is subject to the variable load caused by quick start and stop of the rotor. So, the mechanical response of the joint at high strain rate should be evaluated. However, most of the research work are concerned primarily with discussions of the mechanical response of the brazed joints at low strain rate, such as tensile and shear properties; mechanical response of the brazed joint at high strain rate is seldom discussed.

In our previous work [12], TiAl-based alloy and 42CrMo steel have been successfully vacuum brazed with Ag–Cu/Ti/Ag–Cu multiplayer alloy, the mechanical response of the brazed joint at low strain rate were studied carefully, an optimum joint with tensile strength as high as 347 MPa was acquired. In this work, Mesnager impact tests of the TiAl/steel brazed joints were conducted at room temperature (293 K) and elevated temperature. Utilizing a TiAl turbine/steel shaft structure as the turbine rotor in a car, the TiAl turbine is often under a temperature load up to 873 K, the brazed joint is often under a much lower temperature load up to 623 K because of the oil cooling. So, the elevated test temperature is selected at 623 K. The impact tests of the TiAl base metal were also conducted for

comparing purpose. Impact strength, energy, and fracture path of the joints were studied to evaluate the joint mechanical properties at high strain rate.

Experimental

The materials used in this article were a forged TiAl-based alloy block and a rolled 42CrMo steel bar, the chemical compositions of which were Ti–46.5 Al–2.5 V–1.0 Cr (at.%) and Fe–0.42 C–1.0 Cr–0.7 Mn–0.3 Si–0.5 Mo (wt.%), respectively. The Ag–Cu/Ti/Ag–Cu multilayer filler metal was foil with the thickness of 50 μm and its chemical composition is about Ag–33 Cu–4.5 Ti (wt.%). Bonded surfaces were ground flat by 200 #, 400 #, 600 # grit paper and cleaned in acetone and ethanol prior to brazing process. The filler metal was put between the surface of TiAl alloy and steel. In the previous work [12], the interface structure, formation phases and the microstructure evolution of the brazed joint have been discussed, and the optimum brazing parameters (900 °C/5 min) were obtained. So, in this work the impact specimens of the TiAl/steel joints were brazed at 900 °C for 5 min with a vacuum of 3×10^{-4} Pa.

Figure 1 shows the sketch of a Mesnager impact specimen. For the TiAl base metal, the U-shape notch is just in the middle of the impact specimen. For the TiAl/steel brazed joint, the notch should be precisely cut, so that the arc peak point is just in the middle point of the brazing seam, but this is very difficult. Fortunately, the notch of the Mesnager impact specimen is a U-shaped arc, notch tip effects of which are very weak, this is an important reason that Mesnager impact test but not sharp impact test was chosen. Impact tests were conducted at room temperature (293 K) and elevated temperature (623 K) with an initial impact speed of 5.0 m/s in air using a drop-testing machine (Instron-1190) of 60 J energy capacity. For the room temperature test, the specimen was directly set on the bed of the Mesnager impact testing machine for test; and for the elevated temperature test, the specimen was firstly heated to a fixed temperature (623 K) in an electric furnace and held at this temperature for 0.8 ks in air. Then the specimen was taken out of the furnace and set on the bed of the machine for test. Impact load and impact energy were automatically recorded using the computer software and the average energy and strength were determined for five specimens produced under the same conditions. In order to analyze the fracture path and the crack propagation process, before the impact test the cross sections of brazed joints were ground flat and polished by standard techniques. After the impact test, cross sections of the fractured joints were mounted in an epoxy and prepared for metallographic analysis. The microstructure and fracture path of the cross sections were examined by metallographic microscopy (Neuphi-Olympus), electron probe X-ray microanalysis (EPMA, JXA-8600), scanning electron microscopy (SEM, HITACHIS-47 W).

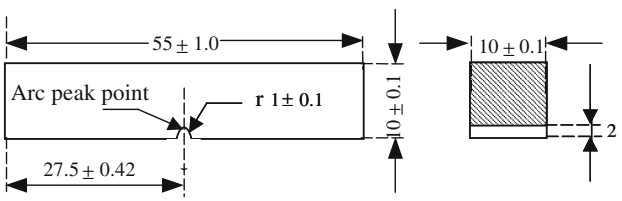

Fig. 1 Sketch of the mesnager impact specimen

Results and discussion

Impact energy and impact strength of the joints and base metal

Figure 2 shows the typical curves for the energy and load versus deflection of the specimens during the Mesnager impact test. During this process, the specimen is subjected to a variable impact load. Initially, the load is smaller and then the load increases gradually and reaches its maximal value and goes down gradually, until the specimen is destroyed completely. However, the impact energy of the specimen increases gradually and reaches its maximal value until the specimen smashes. The load and energy curves show the characters of the specimen when subjected to the impact load. Dynamic energy and maximum loads are determined from the recorded load-deflection curves using a computer device in the instrumented Mesnager impact machine system, where the deflection means the displacement of specimens.

In this article, 10 specimens of the brazed joints and 10 TiAl base metal specimens were prepared for impact test at room and elevated temperature, average energy and strength at each temperature were determined for five specimens.

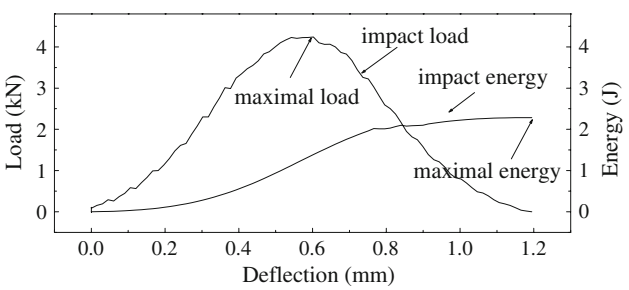

Fig. 2 Typical impact energy and impact load of the specimen during the mesnager impact test

Table 1 Impact load (kN)/impact energy (J) of the TiAl base metal and TiAl/steel brazed joints under impact load at room temperature (RT, 273 K) and elevated temperature (ET, 623 K)

	1	2	3	4	5	Average value
RT joint	4.46/2.51	4.35/2.22	4.24/2.00	4.2/1.99	3.96/1.87	4.25/2.12
RT TiAl	5.72/3.01	5.01/2.99	4.46/2.76	5.01/2.95	5.05/2.96	5.05/2.95
ET joint	3.50/1.66	3.91/2.00	3.75/1.75	3.80/1.98	3.79/1.86	3.75/1.85
ET TiAl	5.33/3.11	4.95/2.93	4.85/2.91	4.98/2.98	4.79/2.87	4.98/2.96

Table 1 shows the mechanical response of the TiAl base metal and TiAl/steel brazed joints under impact load at room temperature and elevated temperature. It can be seen that the average energy and load of the brazed joints are smaller than the TiAl base metal at each temperature. For the room temperature test, the average energy and the load of the brazed joints are 2.12 J and 4.25kN, respectively; and which of the TiAl base metal are 2.95 J and 5.05kN, respectively. For the elevated temperature test, the average energy and the load of the brazed joint are 1.85 J and 3.75kN, respectively; and which of the TiAl base metal are 2.96 J and 4.98kN, respectively. The average impact energy and impact strength of the brazed joints are 71.9% and 84.2% of TiAl base metal at room temperature, respectively; which are 62.5% and 75.3% of the TiAl base metal at elevated temperature, respectively. According to the data above, when the temperature changed in the range from room temperature to 623 K, the impact strength and energy of the TiAl base metal kept on a similar level; however, impact strength and energy of the brazed joints decreased evidently, this may be because of the thermal expansion coefficient differences of TiAl, brazing seam and 42CrMo steel. For supporting the viewpoint above, tensile strength tests of the filler metal were carried out at 293 K and 623 K, and the average tensile strength of the filler metal are 375 MPa and 360 MPa, respectively. According to the tensile test results of the filler metal at different temperature, the strength at 293 K (375 MPa) is nearly equal to the strength at 623 K (360 MPa). So, we consider the thermal expansion coefficient difference of the TiAl, steel and the brazing seam is an important reason for the decrease of the impact strength and energy.

Typical fracture path of the TiAl/steel brazed joint

In the previous work, the interface structure, formation phases, and the microstructural evolution of the joint have been discussed. The typical interface structure could be divided into three distinct zones, as can be seen in Fig. 3: the Al–Cu–Ti reaction layers located near TiAl, composed of Ti_3Al, AlCuTi, and $AlCu_2Ti$ intermetallics; the central zone that consists of a Ag-based solid solution in which Ag–Cu eutectic phase and irregular AlCu2Ti phase are

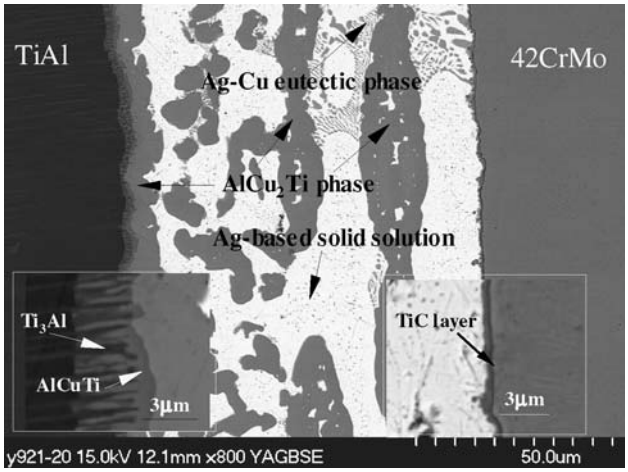

Fig. 3 SEM BEI of the cross-section of the joint brazed at 900 °C for 5 min

dispersed; the TiC layer adjacent to the 42CrMo steel [12]. The fracture path and how these zones and phases behave under impact load should be studied.

Fracture path observation results show that the fracture paths of the brazed joints seem similar at room and elevated temperature. Figure 4a–d shows the typical fracture path of the TiAl/steel brazed joint under impact load. The cracks germinated at the edge of the brazing seam firstly, as can be seen in Fig. 4a; grew and propagated into the Al–Cu–Ti brittle reaction layers near TiAl, as can be seen in Fig. 4b; then propagated into TiAl base metal and resulted in failure. Figure 5 shows the magnified SEM BEIs of the cracks initiation zone in Fig. 4a. It can be seen that the deformation difference of the Ag-based solid solution and the $AlCu_2Ti$ particles induced the cracks germinated at the interface of Ag-based solid solution/ $AlCu_2Ti$ particles.

Although the Al–Cu–Ti intermetallic phase adjacent to the TiAl base metal is brittle, it is a hard phase, and if these kinds of intermetallic reaction layers are not very thick, they are reinforced phases [12–14]. The Ag-rich phase is a ductile phase with $AlCu_2Ti$ particles and Ag–Cu eutectic phase dispersed in it, it is much thicker than the Al–Cu–Ti layer adjacent to the TiAl base metal, and maybe there are

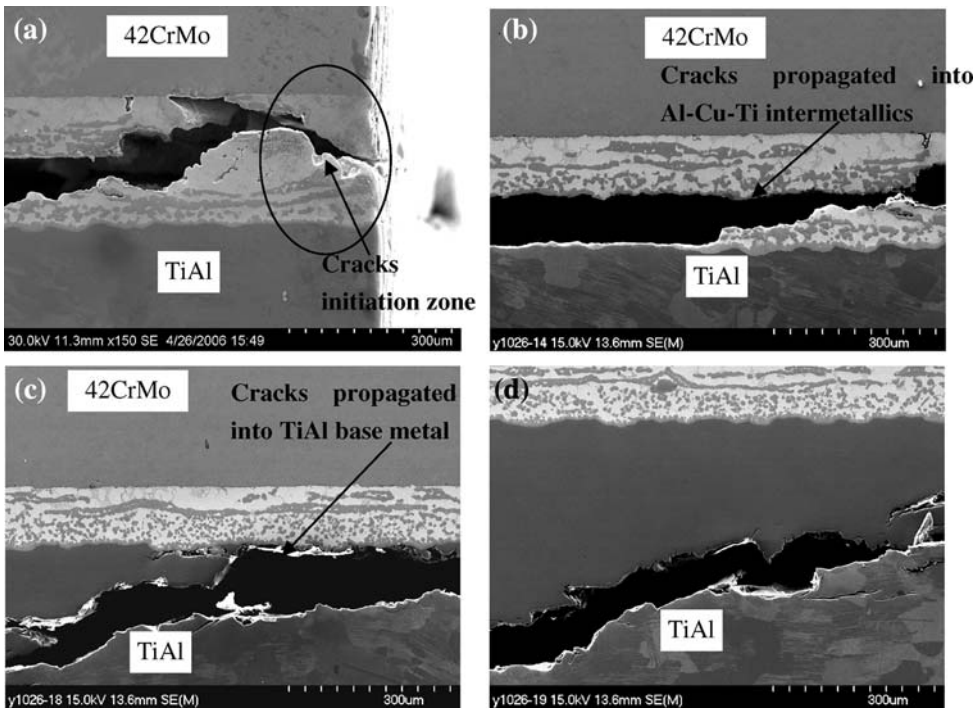

Fig. 4 Typical fracture path of the TiAl/steel brazed joint under impact load

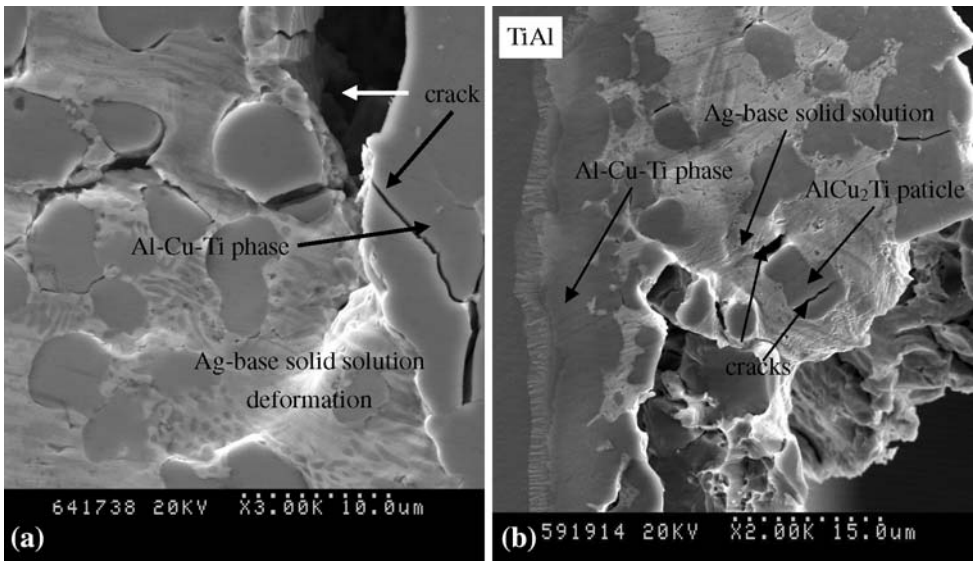

Fig. 5 SEM BEIs of Ag-based solid solution deformation and cracks initiation: **a** crack propagation was prevented by the Ag-base solid solution deformaiont; **b** the region near TiAl base metal

micro-flaws in the Ag-rich phase. When subjected to the impact loads: Ag-based solid solution was deformed quickly, but the $AlCu_2Ti$ particles in it could not be deformed synchronizingly, the deformation difference of the Ag-based solid solution and the $AlCu_2Ti$ particles induced the cracks germinated at the interface of Ag-based solid solution/$AlCu_2Ti$ particles. So, it seems that the crack initiates from the ductile Ag-rich matrix but not from the brittle Al–Cu–Ti layer adjacent to the TiAl base metal.

The impact value of TiAl substrate is higher than that of TiAl/steel joint; however, the TiAl alloy is also a hard and brittle phase. Especially, when it has been brazed, the region adjacent to the brazing seam becomes much weaker than before brazing. The Al–Cu–Ti intermetallic layer is much thinner than the TiAl base metal. So, it is comprehensible that the crack propagates along the layer of Al–Cu–Ti layer, then enters into the TiAl substrate when the specimen was distorted by the impact load and finally the specimen is fractured in TiAl substrate.

According to Figs. 4 and 5, the phases in the brazing seam behaved differently when subjected to the impact loads: Ag-based solid solution was deformed quickly,

although the cracks germinated at the interface of Ag-based solid solution and the $AlCu_2Ti$ particles, the cracks were prevented propagating in the brazing seam by the deformation of this soft phase; $AlCu_2Ti$ particles prevent the deformation of the Ag-based solid solution, and sometimes cracks could germinate in an $AlCu_2Ti$ strip phase; the cracks propagate easily in the Al–Cu–Ti ternary intermetallics near the TiAl base metal; although the TiC phase is a hard phase, it seemed this phase have no relations to the crack initiation and propagation.

Conclusion

Mesnager impact tests of the TiAl/steel brazed joints were conducted at room temperature (293 K) and elevated temperature (623 K). Impact strength, energy, and fracture path of the joints were studied to evaluate the joint mechanical properties under high strain rate. The primary conclusions can be summarized as below:

(1) For room temperature test, the average impact energy and impact strength of the brazed joint are 71.9% and 84.2% of the TiAl base metal, respectively; which are 62.5% and 75.3% of the TiAl metal at elevated temperature (623 K), respectively.
(2) The phases in the brazing seam behaved differently when subjected to the impact loads: Ag-based solid solution was deformed quickly, and the cracks propagation in the brazing seam were prevented by the deformation of this phase; $AlCu_2Ti$ particles prevent the deformation of the Ag-based solid solution; the cracks propagate easily in the Al–Cu–Ti ternary intermetallics near the TiAl base metal; the TiC layer near 42CrMo steel had no relations to the crack initiation and propagation.
(3) The joint fracture path analysis show, when subjected to the impact load, minute cracks germinate at the interface of Ag-based solid solution/$AlCu_2Ti$ particles, then the cracks grew and propagated into the Al–Cu–Ti brittle reaction layers and TiAl base metal, and resulted in failure.

Acknowledgements The authors should gratefully acknowledge the financial support from National "973" Foundation Pre-Program of China (No.2005CCA04300), the Natural science foundation of JiangXi province (No.2008GQC0013), and the State Key Lab of Advanced Welding Production Technology, Harbin Institute of Technology.

References

1. Lee SJ, Wu SK, Lin RY (1998) Acta Mater 46:1283
2. Çam G, İpekoğlu G, Bohm KH et al (2006) J Mater Sci 41:5273. doi:10.1007/s10853-006-0292-4
3. Clemens H, Kestler H (2000) Adv Eng Mater 2:551
4. Shiue K, Wu SK, Chen SY (2004) Intermetallics 12:929
5. Tetsui T (2002) Mater Sci Eng A 329–331:582
6. Noda T (1998) Intermetallics 6:709
7. Appel F, Brossmann U, Christoph U et al (2000) Adv Eng Mater 2:699
8. Draper SL, Krause D, Lerch B (2007) Mater Sci Eng A 464:330
9. Noda T, Shimizu T, Okabe M et al (1997) Mater Sci Eng A 239–240:613
10. Lee WB, Kim YJ, Jung SB (2004) Intermetallics 12:671
11. Lee WB, Kim MG, Koo JM (2004) J Mater Sci 39:1125. doi: 10.1023/B:JMSC.0000012960.59095.5a
12. Li YL, He P, Feng JC (2006) Scripta Mater 55:171
13. Çam G, Özdemir U, Ventzke V et al (2008) J Mater Sci 43:3491. doi:10.1007/s10853-007-2403-2
14. Liu HJ, Feng JC (2002) J Mater Sci Lett 21:9